Progress In Electromagnetics Research M, Vol. 120, 145–154, 2023

Measurement and Prediction of Signal Strength of Wireless Sensor Network

Li Yang Foong, Soo Yong Lim*, and Kheong Sann Chan

Abstract—This paper utilizes an efficient prediction model using the concept of ray-tracing based on the Theory of Geometrical Optics (GO) to predict the signal strength between two wireless sensor nodes within an indoor environment, which can provide aid to designers in the implementation of Wireless Sensor Networks (WSNs). WSN is a technology that is widely used for functions such as collecting and processing data, then transmitting it wirelessly within the network. WSNs are typically autonomous and self-organizing networks of nodes that communicate wirelessly with each other and collaborate to perform tasks such as data processing, sensing, aggregation, and forwarding. With the increasing prevalence of WSNs in indoor environments, installations of numerous sensor nodes are necessary to collect and transmit data in certain areas, which builds up to a single network. Thus, to ensure the functionality of the WSNs, it is of utmost importance to ensure a reliable connection between the nodes, which is directly affected by its location and placement. The prediction model developed in this work is built using MATLAB software, which is then implemented into a Graphical User Interface (GUI) using MATLAB App Designer, which allows modifications to be made to the prediction model as to fit the user's environment. The results of our prediction model are compared against experimental ones obtained through physical measurements using wireless communications technologies such as ZigBee and Bluetooth Low Energy (BLE).

1. INTRODUCTION

Wireless Sensor Network (WSN) is a network of sensor nodes that monitors the physical or environmental conditions of a given region by deploying multiple sensor nodes across the said region. This enables the sensor network to perform many functions in an industrial setting such as sensing/data acquisition, data processing, data communication, data forwarding, data fusion and aggregation, localization and tracking, monitoring and control [1–3]. With the increasing prevalence of WSN, considerations need to be taken in determining the locations of the sensor nodes, as many factors should be considered such as the suitability of the location in collecting specified data, the operational range of the sensor nodes, and most importantly the stability of the connection between sensor nodes so that they are able to reliably transmit and receive data between the nodes. Thus, the locations of the sensor nodes need to be optimized such that it is able to achieve the largest combined operational range while maintaining a reliable connection between nodes [4, 5].

In order to predict the signal strength between two nodes, the Ray Tracing method has been used to determine the ray path to calculate the final signal strength between the two nodes at any given inter-node distance. To verify the accuracy of the prediction models, physical measurements were performed to collect the Received Signal Strength Indicator (RSSI) values between the two nodes at the given points, where wireless communication protocols such as ZigBee and Bluetooth Low Energy (BLE) were used to collect a larger variety of data [6].

Received 3 July 2023, Accepted 25 October 2023, Scheduled 3 November 2023
* Corresponding author: Soo Yong Lim (Grace.Lim@nottingham.edu.my).
The authors are with the University of Nottingham Malaysia, Malaysia.

2. EXPERIMENTAL SETUP

Two situations are considered in this work, both of them being indoor corridors. The first one is a straight corridor where both nodes have a direct line-of-sight link regardless of the nodes' positions along the corridor. The second environment is an L-shape corridor where the two nodes will lose the direct line-of-sight link between each other. Two wireless communication technologies, ZigBee and BLE, were used to perform the physical measurements. The wireless modules used are the ZigBee XBee S2 module and HM-10 BLE module. The XBee S2 module has a omnidirectional wire antenna with a transmitting power of 5 dBm, and the HM-10 module has a omnidirectional printed circuit board (PCB) trace antenna with a transmitting power of 0 dBm. Both modules operate in the 2.4 GHz Industrial, Scientific, and Medical (ISM) band. These technologies were chosen due to the ability of ZigBee WSN to cover large areas or between buildings, as well as their low cost and low power consumptions. Meanwhile, the BLE WSN is a commonly used technology for smaller area connections such as smart home applications, which also have extremely low power consumption and cost [7–11].

To setup the physical measurements for ZigBee XBee S2 modules, one of the modules is set as the coordinator node and the other as the router node. This can be done by connecting the ZigBee modules to a laptop via the USB port and utilizing the Digi International X-CTU software. To wirelessly connect the two modules, the PAN ID and Scan Channels (SC) values of both modules should be identical, and in the addressing section, the Serial High and Serial Low ID of the coordinator should be placed in the Designated High and Designated Low of the router, and vice versa. Furthermore, the X-CTU software offers a range testing function, which can effectively display the RSSI values between the two nodes at any given time and position as long as the nodes are wirelessly connected to one another. The connections of the coordinator node and router node are shown in Figure 1, where the coordinator node acts as the transmitter and is connected to the laptop, and the router node acts as the receiver and is connected to a 9 V battery so that it is portable.

To set up the HM-10 BLE modules, each module is connected to an Arduino Uno which is in turn connected to a laptop via USB and configured using the Arduino IDE with AT commands. Using AT+ROLE the first module will be set as the master node, and the other module will be the slave node. With AT+IMME1 the modules will prevent automatic connections, and lastly using AT+DISC? sent by the master module, the RSSI values between the nodes at the given time will be generated. The experimental setup of both modules are shown in Figure 2, where the master node is connected to a laptop and acts as the transmitter, and the slave node is connected to a 9 V battery and acts as a portable receiver.

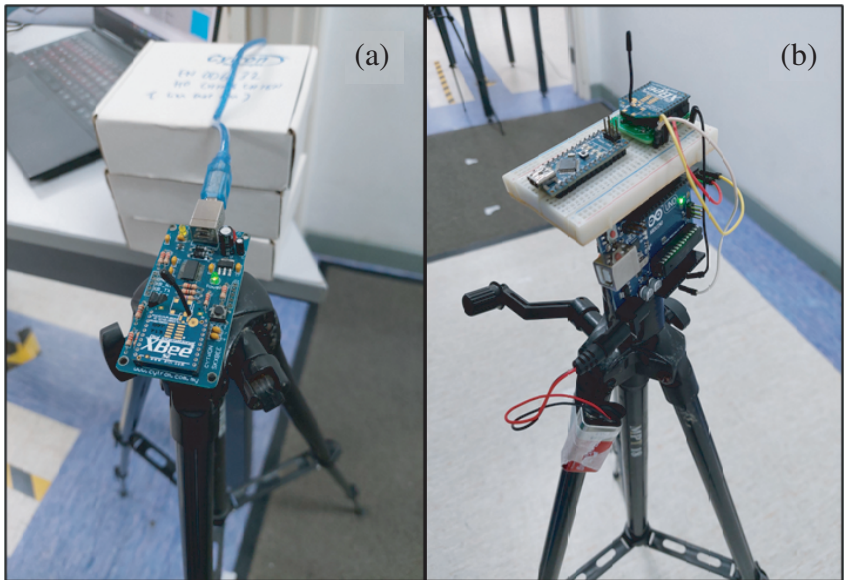

Figure 1. Experimental setup for XBee S2 modules. (a) Coordinator node. (b) Router node.

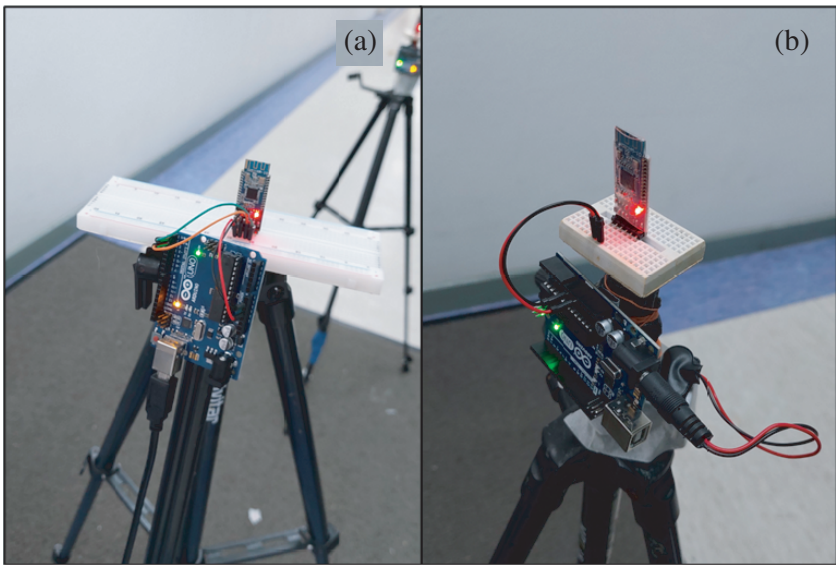

Figure 2. Experimental setup for HM-10 BLE modules. (a) Master node. (b) Slave node.

2.1. Straight Corridor

The straight corridor selected has a height of 3 meters, a width of 1.868 meters, and a total length of 36 meters. The two walls of the corridor also consist of different materials such as glass panels and doors. The nodes are placed at the center of the corridor, at a height of 0.92 meters. The coordinator node or the master node is placed at the start of the corridor and is connected to a laptop via USB, while the router node or the slave node is moved down the corridor. Every 0.5 meters, the RSSI value between the two nodes is recorded until the router node or slave node reaches the end of the corridor. A pictorial representation and experimental setup is shown in Figure 3.

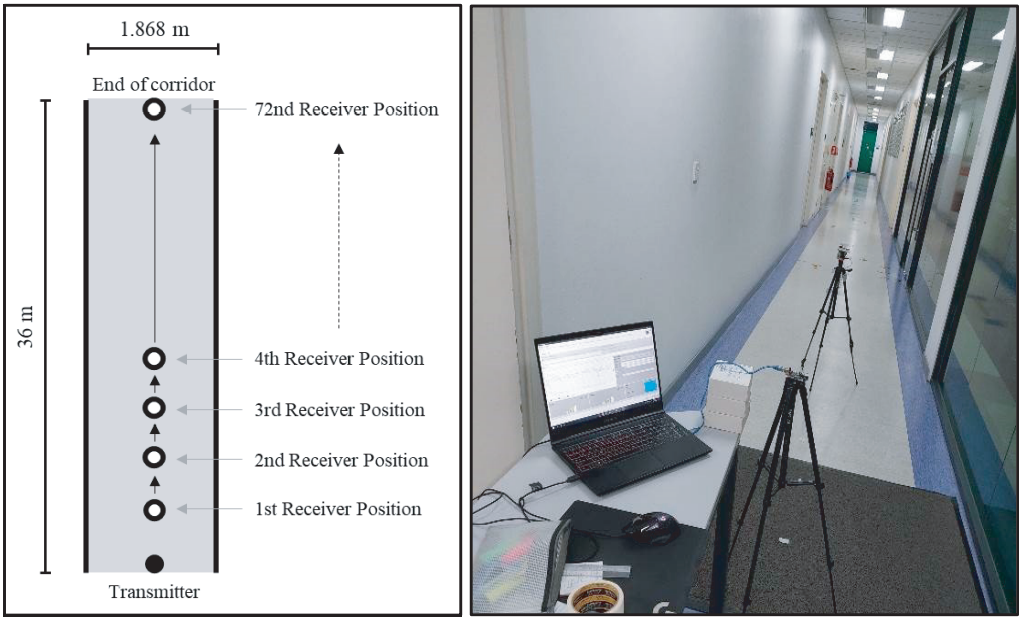

Figure 3. Straight corridor experimental setup.

2.2. L-Shape Corridor

The selected L-shaped corridor consists of two connected corridors where both the width and length of the two corridors are different. A pictorial representation of the L-shaped corridor is shown in Figure 4.

For the shorter corridor, it has a height of 3 meters and width of 1.65 meters, with its total length of 6 meters. The longer corridor has a height of 3 meters and width of 2.27 meters, with its length being 25 meters. As depicted in Figure 4, the coordinator node or master node is placed at the start of the shorter corridor, while the router node or slave node moves along the length of the longer corridor in steps of 0.5 meters, which causes the nodes to lose its line-of-sight link. The RSSI value between the two nodes is recorded every 0.5 meters until the router node reaches the end of the longer corridor.

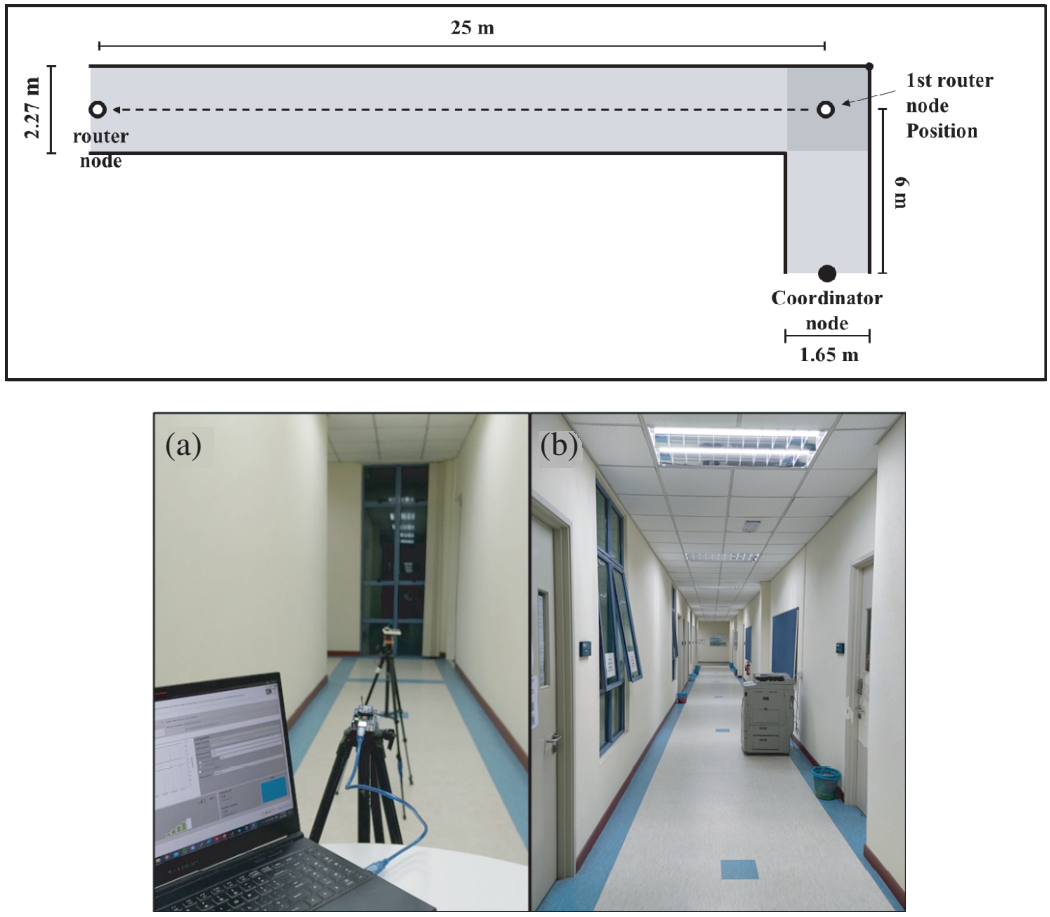

Figure 4. L-Shape Corridor. (a) Shorter corridor. (b) Longer corridor.

3. RAY-TRACING PREDICTION MODELS

We have utilized the ray-tracing image method to do the prediction of signal strength. This method is based on Fermat's principal of least time, where the ray takes the route that spends the least amount of time as it travels from one point to another [12, 13]. Figures 5 and 6 show the occurrence of a first and second order reflection in the implementation of the image method, where R represents the receiver (or router) node, and T is the transmitter (or coordinator) node. T' is the first image of T reflected on the upper wall, and T" is the second image of T' reflected on the lower wall. By drawing a line from the second image T" to R, the second point of reflection can be determined as the intersection of this ray with the wall, and the first point of reflection can be determined by connecting the second point

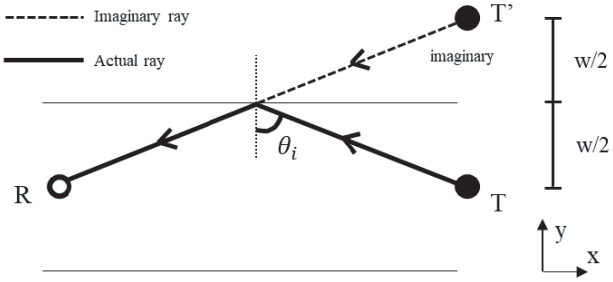

Figure 5. Ray-tracing image method (first order reflection).

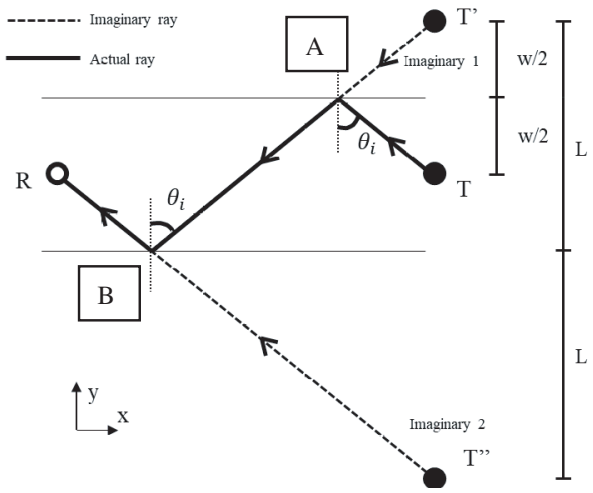

Figure 6. Ray-tracing image method (2nd order reflection).

of reflection to T'. The order of reflections can be increased arbitrarily, by increasing the number of imaginary transmitters in each reflecting surface.

The prediction model for the straight corridor is created using MATLAB, and it is assumed that the corridor walls have the same depth; the ceiling and floor are uniform and flat; lastly, there are no obstacles along the corridor. Regarding the reflected rays, up to the third order of reflections are considered in our simulation. Considering the different materials present in the walls of the corridor, the dimensions of the walls for the straight corridor are measured and recorded, and the materials are then assumed to obtain the corresponding relative permittivity displayed in Table 1.

Table 1. Relative Permittivity of materials.

Materials	Relative Permittivity ε_r
Concrete	4.5
PVC	4.0
Glass	5.0
Wood	5.0

The line-of-sight (LoS) ray is the direct ray transmitted from the transmitter to the receiver. The electric field equation for path loss of LoS ray is written as

$$E_{LOS} = \frac{1}{r} e^{-j\beta r} \tag{1}$$

where r is taken as the distance that the ray path travels from the transmitter to reach the receiver while adhering to the Fermat's principle of least time, and β is the wave number given as $\frac{2\pi}{\lambda}$. In the case of Eq. (1), the line of sight scenario, the ray path is drawn directly from the transmitter to the receiver.

The first order reflection of a ray is a ray that is reflected once on any interface before reaching the receiver. By applying the ray tracing of image method, the point of reflection on the interface can be determined. As shown in Figure 5, for a first order reflected ray, the transmitter is reflected once over the interface. An imaginary line is connected from the reflected transmitter image to the receiver. The point of intersection of the imaginary line and interface is the point where the transmitted ray hits and

bounces off the receiver. The electric field equation for path loss of first order reflection is written as

$$E_{r1} = \Gamma \frac{1}{r} e^{-j\beta r} \tag{2}$$

where Γ is the reflection coefficient. $\Gamma = \Gamma_{\parallel} = \frac{\eta_2 \cos\theta_t - \eta_1 \cos\theta_i}{\eta_2 \cos\theta_t + \eta_1 \cos\theta_i}$ is used for parallel polarization (ground reflection), and $\Gamma = \Gamma_{\perp} = \frac{\eta_2 \cos\theta_i - \eta_1 \cos\theta_t}{\eta_2 \cos\theta_i + \eta_1 \cos\theta_t}$ is used for perpendicular polarization (wall reflection), where θ_i is the incident angle, θ_t the transmitted angle, and η the impedance given as $\sqrt{\frac{j\omega\mu}{\sigma + j\omega\varepsilon}}$, where μ, σ, and ε are the permeability, conductivity, and permittivity, respectively [14]. The r in Eq. (2) now refers to the distance along the zig-zag path from the transmitter to the receiver. Alternatively, this distance can be taken from the image of the transmitter to the receiver.

For multiple reflections, multiple reflected images with respect to the relevant interfaces are determined in a similar way as the first order reflection to obtain the corresponding ray paths. Figure 6 shows an example of multiple reflections, which is the second order reflection of ray. From Figure 6, after performing the first order reflection of transmitter as shown in Figure 5, the transmitter image T' is reflected again to obtain the transmitter image of second order reflection, T". The point of intersection between the interface and the imaginary line connecting T" and receiver is the point where the ray is reflected for the second time. The point of intersection between the previous point of intersection and the first order transmitter image T' is the first point where the ray hits and bounces off. Hence, the ray trajectory for second order reflection of ray shown in Figure 6 is from T to A to B to R.

The electric field for path loss of second order reflection is modelled as

$$E_{r2} = \Gamma_1 \Gamma_2 \frac{1}{r} e^{-j\beta r} \tag{3}$$

where Γ_1 is the reflection coefficient of the first order reflection, and Γ_2 is the reflection coefficient for the second order reflection of the ray. The reflection coefficients of the respective orders will be multiplied to the electric field equation as the order of reflection increases. In our work, we have considered up to third order reflections. For extra rays such as that from diffraction, it can be further factored in following the principles laid out in [15].

The total electric field at a point is the sum of the line of sight and each reflected ray and is given as

$$E_{total} = E_{LOS} + \sum E_r \tag{4}$$

Finally, the path gain equation is obtained by

$$PG = 20 \log(|E_{total}|) \tag{5}$$

4. GRAPHICAL USER INTERFACE (GUI)

To provide a more efficient and convenient method to utilize the respective prediction models, a Graphical User Interface (GUI) was thought to be a suitable platform where the user would be able to configure certain parameters of the prediction model itself for it to better suit their application. Designed using the App Designer in MATLAB, the GUI will also display the ray-tracing performance so that the user is able to visualize the bouncing of rays.

As shown in Figure 7, the GUI for the straight corridor consists of many functions such as displaying the bouncing rays at a given point, displaying the coordinates where reflection occurs, outputting the signal strength (dBm) between the two nodes at the given point, generating the signal strength graph along the corridor, changing locations of the coordinator node and router node, and configuring the environment, which links to a sub-app that has the flexibility of modifying the dimensions of the corridor itself shown in Figure 8.

5. RESULTS

In this section, we present the measurement and prediction results in the two scenarios. Figure 9 shows that the ZigBee modules have less variations in the measured RSSI values, and BLE modules have more

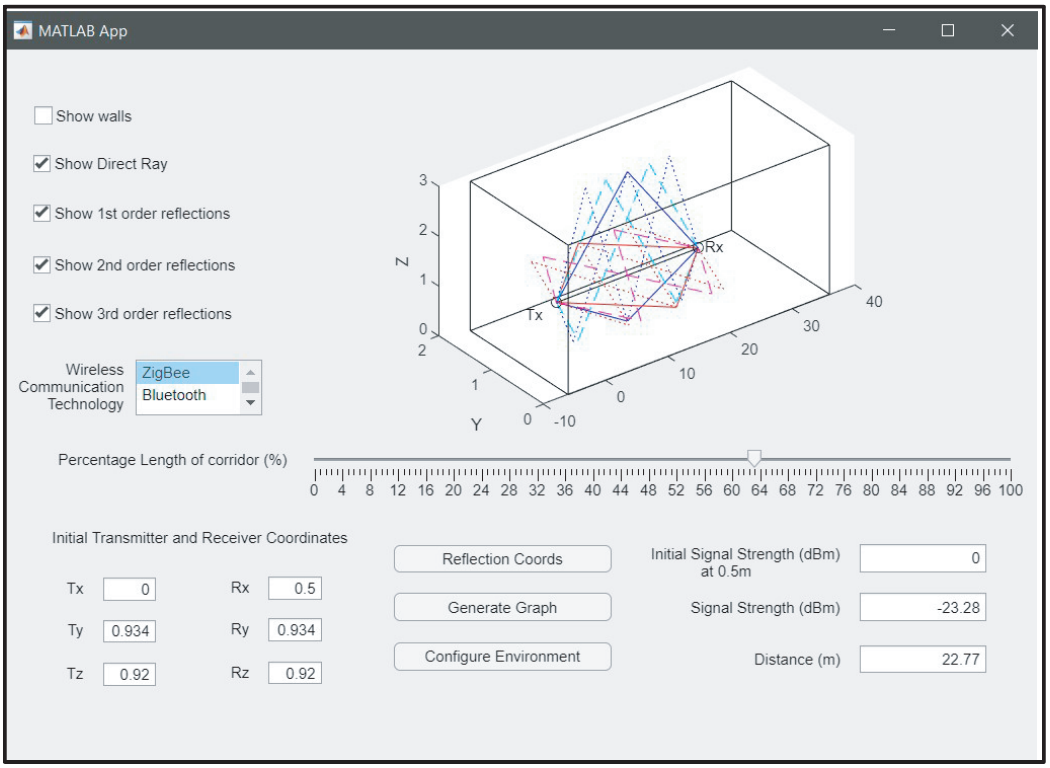

Figure 7. Straight Corridor GUI.

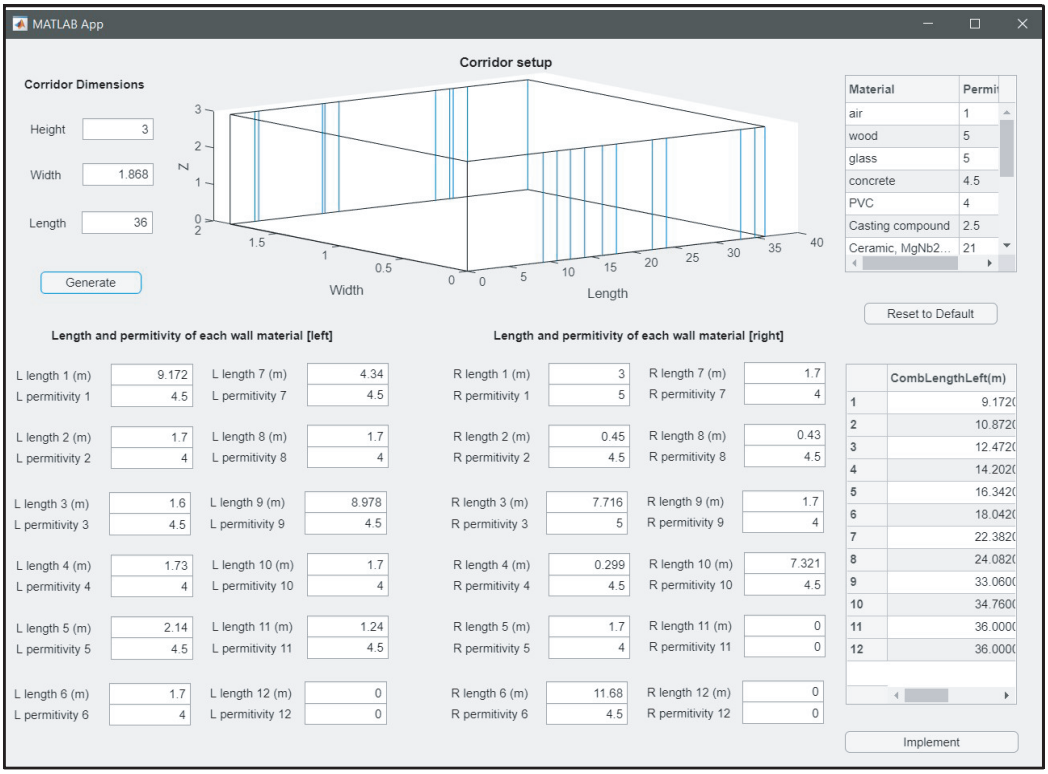

Figure 8. Configure Environment Sub-App.

variations in the measured RSSI values. The overall values of the signal strength of BLE are also lower than ZigBee, which is mainly due to BLE modules having a shorter operational range than ZigBee modules.

Figure 10 shows that the measured RSSI values of the BLE modules in the L-shape corridor are once again lower than the measured RSSI values of the ZigBee modules, and as the router node moves along the longer corridor it loses the line-of-sight link from the coordinator node, so the signal strength values are generally lower than the values in Figure 9. Furthermore, according to IEEE 802.15.4 standard the lowest signal strength value that can provide a reliable connection between wireless modules is -85 dBm, which indicates that the HM10 BLE modules are unsuitable to be applied in this L-shape corridor [16].

In Figure 11, the overall pattern of the MATLAB results matches the RSSI measurements of both ZigBee and BLE, where the BLE average RSSI has a better match than the ZigBee average RSSI. The root-mean-square error (RMSE) between the prediction model results and the average RSSI for ZigBee XBee modules is 5.0413, and the RMSE between the prediction model results and the average RSSI for HM-10 BLE modules is 4.0652. In this case, the antenna gain of the wireless modules is not as

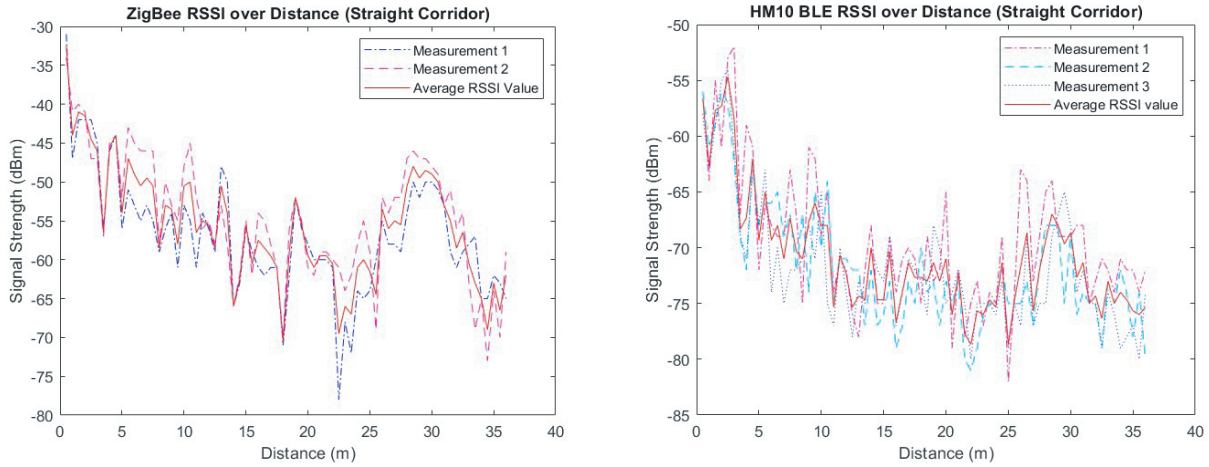

Figure 9. Straight Corridor RSSI measurements. (a) ZigBee. (b) BLE.

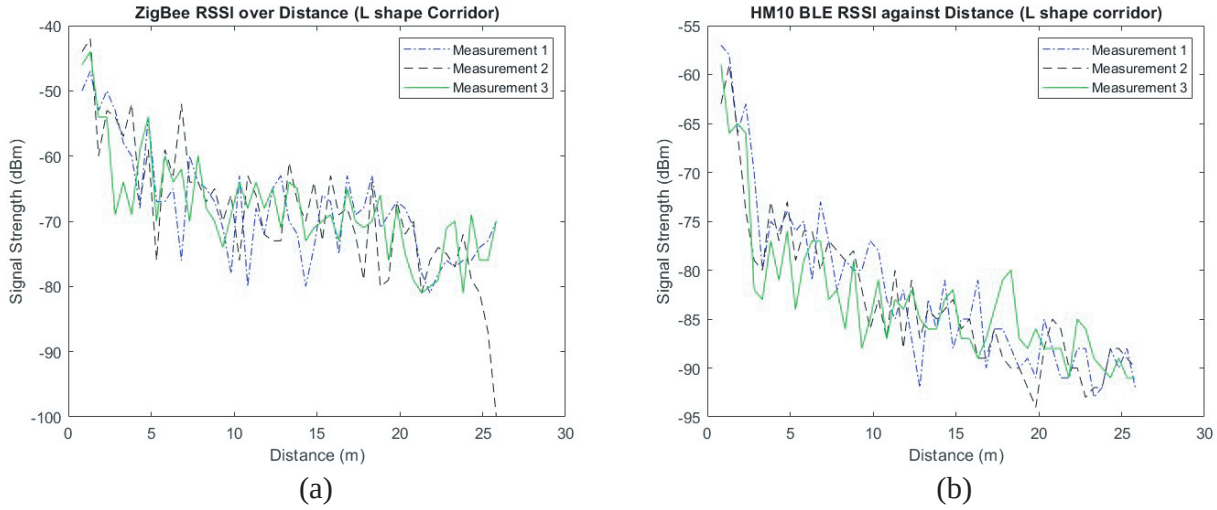

Figure 10. L Shape corridor RSSI measurements. (a) ZigBee. (b) BLE.

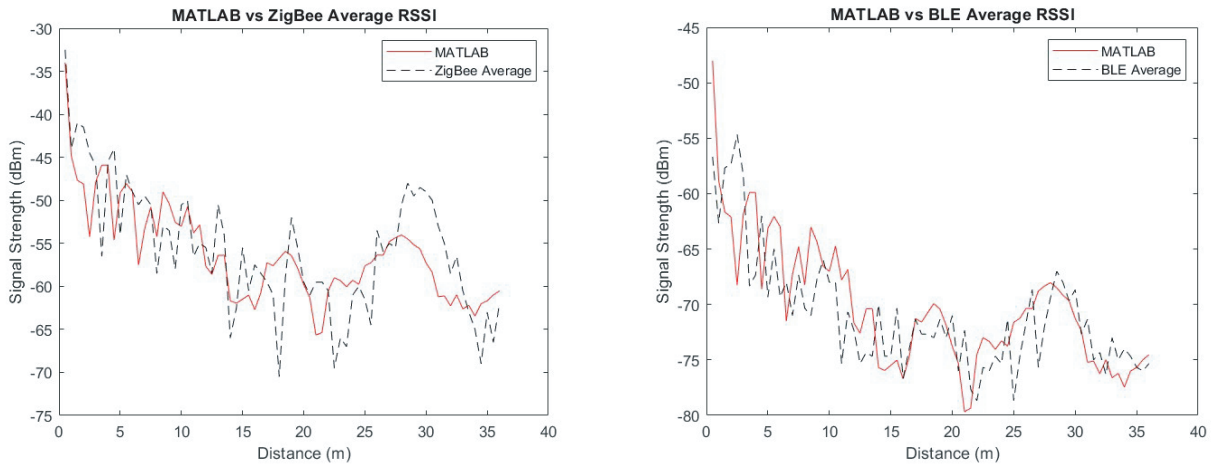

(a) (b)

Figure 11. Straight Corridor Prediction model results. (a) ZigBee. (b) BLE.

relevant as the prediction model results have been shifted to match the measured results of the average RSSI of both ZigBee and BLE. The main purpose of the prediction model is to predict the trend of the signal strength along the corridor, hence our goal is to examine this trend. We have placed the antenna vertically polarized with respect to the ground, and the amplitude computed at each point in this figure is the summation of all ray paths, with its value taken as log10, and multiplied with 20, as stated in Eq. (5).

6. CONCLUSION

This paper has presented an efficient method to obtain the signal strength within an indoor corridor using the ray-tracing image method in a prediction model, where its results for the straight corridor is reasonably accurate in comparison with the RSSI values obtained from physical measurements. Furthermore, a GUI has been designed utilizing these prediction models to further improve its robustness that can be used for different environments. The results obtained from this work contribute towards ensuring the functionality of WSN, which relies heavily on reliable connection between the nodes.

REFERENCES

1. Kocakulak, M. and I. Butun, "An overview of Wireless Sensor Networks towards internet of things," *2017 IEEE 7th Annual Computing and Communication Workshop and Conference (CCWC)*, 1–6, Las Vegas, NV, USA, 2017, doi: 10.1109/CCWC.2017.7868374.
2. El-Maghrabi, H. M., "A standard ray tracing technique for predicting signal strength of wireless sensor network in smart building," *Progress In Electromagnetics Research Letters*, Vol. 105, 79–84, 2022.
3. Ashok Somani, N., "Zigbee: A low power wireless technology for industrial applications," *Int. J. Control Theory Comput. Model.*, Vol. 2, No. 3, 27–33, May 2012, doi: 10.5121/ijctcm.2012.2303.
4. Mahmood, M. A., W. K. G. Seah, and I. Welch, "Reliability in wireless sensor networks: A survey and challenges ahead," *Comput. Networks*, Vol. 79, 166–187, Mar. 2015, doi: 10.1016/j.comnet.2014.12.016.
5. Kurt, S. and B. Tavli, "Path-loss modeling for wireless sensor networks: A review of models and comparative evaluations," *IEEE Antennas and Propagation Magazine*, Vol. 59, No. 1, 18–37, Feb. 2017, doi: 10.1109/MAP.2016.2630035.

6. Laaraiedh, M., et al., "Ray tracing-based radio propagation modeling for indoor localization purposes," *2012 IEEE 17th International Workshop on Computer Aided Modeling and Design of Communication Links and Networks, CAMAD 2012*, 276–280, 2012, doi: 10.1109/CAMAD.2012.6335350.
7. Ramya, C. M., M. Shanmugaraj, and R. Prabakaran, "Study on ZigBee technology," *ICECT 2011 — 2011 3rd International Conference on Electronics Computer Technology*, Vol. 6, 297–301, 2011, doi: 10.1109/ICECTECH.2011.5942102.
8. Vishnubhotla, R., et al., "ZigBee based multi-level parking vacancy monitoring system," *2010 IEEE International Conference on Electro/Information Technology*, 1–4, Normal, IL, USA, 2010, doi: 10.1109/EIT.2010.5612133.
9. Sakphrom, S., K. Suwannarat, R. Haiges, and K. Funsian, "A simplified and high accuracy algorithm of RSSI-based localization zoning for children tracking in-out the school buses using bluetooth low energy beacon," *Informatics*, Vol. 8, No. 4, Dec. 2021, doi: 10.3390/informatics8040065.
10. Nair, K., J. Kulkarni, M. Warde, et al., "Optimizing power consumption in iot based wireless sensor networks using Bluetooth Low Energy," *Proceedings of the 2015 International Conference on Green Computing and Internet of Things, ICGCIoT 2015*, 589–593, Jan. 2016, doi: 10.1109/ICGCIoT.2015.7380533.
11. Darroudi, S. M. and C. Gomez, "Bluetooth low energy mesh networks: A survey," *Sensors (Switzerland)*, Vol. 17, No. 7, MDPI AG, Jul. 01, 2017, doi: 10.3390/s17071467.
12. Lim, S. Y., Z. Yun, and M. F. Iskander, "Radio propagation modeling: A unified view of the ray-tracing image method across emerging indoor and outdoor environments," *The World of Applied Electromagnetics*, 301–328, Springer International Publishing, Cham, 2018.
13. Yun, Z. and M. F. Iskander, "Ray tracing for radio propagation modeling: Principles and applications," *IEEE Access*, Vol. 3, 1089–1100, Institute of Electrical and Electronics Engineers Inc., 2015, doi: 10.1109/ACCESS.2015.2453991.
14. Iskander, M. F., "Oblique incidence plane wave reflection and transmission," *Electromagnetic Fields and Waves. Prospect Heights*, 436–479, Waveland Pr Inc., Illinois, 2000.
15. Zhang, Y. and S. Y. Lim, "An Investigation into the diffraction effects of building FAÇADE for propagation modelling," *Progress In Electromagnetics Research M*, Vol. 97, 25–34, 2020.
16. "IEEE standard for low-rate wireless networks," *IEEE Std 802.15.4-2020 (Revision of IEEE Std 802.15.4-2015)*, 1–800, 2020.